Astron. Astrophys. 330, 155–168 (1998)

ASTRONOMY AND ASTROPHYSICS

Multiwavelength optical observations of chromospherically active binary systems

II. EZ Pegasi⋆

D. Montes, J. Sanz-Forcada, M.J. Fernández-Figueroa, E. De Castro, and A. Poncet

Departamento de Astrofísica, Facultad de Físicas, Universidad Complutense de Madrid, E-28040 Madrid, Spain (dmg@astrax.fis.ucm.es)

Received 28 May 1997 / Accepted 17 September 1997

Abstract. The star EZ Peg, long ago classified as cataclysmic variable, has been shown to be a chromospherically active binary system of the RS CVn-type. In this paper we have analysed, using the spectral subtraction technique, simultaneous spectroscopic observations of the Hα, Hβ, Na I D_1 and D_2, He I D_3, Mg I b triplet, Ca II H & K, and Ca II infrared triplet lines. We have found that the hot component is the active star of the system, showing strong emission in the Hα, Ca II H & K, Hϵ, and Ca II IRT lines, and a strong filling-in of the Hβ line, however the Na I D_1 and D_2 and Mg I b triplet lines do not present filled-in. The He I D_3 could present a total filling-in due to microflaring. The observed variations (in different epochs and with the orbital phase) of the different activity indicators, formed at different height in the chromosphere, are correlated. Very broad wings have been found in the subtracted profiles of Hα and Ca II IRT λ8498 and λ8662 lines. These profiles are well matched using a two-component Gaussian fit (narrow and broad) and the broad component could be interpreted as arising from microflaring. The higher luminosity class of the hot component, that our spectra seem to indicate, could explain why the hot component is the active star of the system.

Key words: stars: activity – stars: binaries: close – stars: chromospheres – stars: late-type – stars: individual: EZ Peg

1. Introduction

EZ Peg (BD +24° 4742) has a misleading history of confused interpretation of the origin and composition of the system. The spectrum of EZ Peg was originally classified by Cannon as G5 (Schlesinger et al. 1934). Vyssotsky & Balz (see Alden 1958) claimed that the star varies from B0 to G5, due to a spectrum taken in 1943 which appeared to be a B star spectrum. Later Howell & Bopp (1985) presented evidence that this erroneous interpretation of the spectrum was due to poor resolution data. Irvine (1972) proposed that EZ Peg was an U Gem system (a cataclysmic variable), but it is an unlikely explanation due to the normal UV emission of the system: in a color-color plot there is no strong UV excess typical of the dwarf novae and symbiotics (Szkody 1977). Furthermore linear polarimetry measurements of the system (Szkody et al. 1982) show that EZ Peg does not seem to be a cataclysmic variable.

Howell & Bopp (1985) observed the double-lined spectrum of EZ Peg and interpreted the color-indices (B-V) and (U-B) as that of a composite spectral type of G5 IV + K0 IV. They observed Ca II H & K, Hα and Hϵ lines in emission, and they supposed that this emission originated in the cooler star, because it is the most typical case. Howell et al. (1986) suggested that both components of EZ Peg were subgiants, and pointed out a slightly asymmetric profile in Hα, interpreted as a vertical motion in the atmosphere of the active star of the system.

Griffin (1985) presented radial-velocity observations of the system, and he calculated the orbital elements. Recently Gunn et al. (1996) made cross-correlation radial velocity measurements of EZ Peg, showing a disagreement with the phases calculated from the ephemeris given by Griffin (1985). Vilkki et al. (1986) calculated a distance to EZ Peg of 83 pc using the trigonometric parallax method, and they suspected that EZ Peg belongs to the Hyades cluster. Barret (1996) calculated a distance of 82 pc using linear polarimetry.

Finally, recent studies in the IR band by Mitrou et al. (1996) with the IRAS satellite indicated that the system does not seem to present any circumstellar matter.

Continuing with the series of multiwavelength optical observations of chromospherically active binaries (Montes et al. 1997b, hereafter Paper I), in this paper we present simultaneous observations in different optical wavelength bands, including

Send offprint requests to: D. Montes

⋆ Based on observations made with the Isaac Newton, William Herschel and Jacobus Kapteyn telescopes operated on the island of La Palma by the Royal Greenwich Observatory at the Spanish Observatorio del Roque de Los Muchachos of the Instituto de Astrofísica de Canarias

Table 1. Observing log

Date	IDS-INT												UES-WHT		
	Hα			Na I D_1, D_2, He I D_3			Ca II H & K			Hβ			Echelle		
	UT	φ	S/N	UT	φ	S/N	UT	φ	S/N	UT	φ	S/N	UT	φ	S/N
1993/07/31	-	-	-	-	-	-	-	-	-	-	-	-	02:05	0.954	315
1995/09/14	00:36	0.416	295	00:04	0.414	362	-	-	-	-	-	-	-	-	
1995/09/15	00:23	0.501	332	00:02	0.500	343	-	-	-	-	-	-	-	-	
1996/11/26	21:25	0.141	295	-	-	-	23:11	0.148	295	-	-	-	-	-	
1996/11/27	20:39	0.224	295	20:49	0.225	362	19:35	0.220	295	-	-	-	-	-	
1996/11/28	19:24	0.306	295	20:25	0.310	362	21:44	0.314	295	21:19	0.312	362	-	-	

also a high resolution echelle spectrum. All the data seem to point out that EZ Peg is a RS CVn system with an evolved G5 active star, and a K0V or IV non-active star. We have applied the spectral subtraction technique, observing the Ca II H & K, Hϵ, Hα and Ca IR triplet lines in emission, and a filling-in of the Hβ line, proceeding from the hotter component of the system.

In Sect. 2 we give the details of our observations and data reduction. In Sect. 3 we discuss some of the stellar parameters of the binary system and in Sect. 4 the behavior of the different chromospheric activity indicators is described. Finally in Sect. 5 we present the conclusions.

2. Observations and data reduction

Spectroscopic observations of EZ Peg in several optical chromospheric activity indicators have been obtained during two observing runs with the 2.5 m Isaac Newton Telescope (INT) at the Observatorio del Roque de Los Muchachos (La Palma, Spain) using the Intermediate Dispersion Spectrograph (IDS). In the first run (September 13-15 1995) we have obtained two spectra: in the Hα and Na I D_1, D_2, He I D_3 line regions, using grating H1800V, camera 500 and a 1024 x 1024 pixel TEK3 CCD as detector. The reciprocal dispersion achieved is 0.24 Å/pixel which yields a spectral resolution of 0.48 Å and a useful wavelength range of 250 Å centered at 6563 Å (Hα) and 5876 Å (HeI D_3) respectively. In the second run (November 26-28 1996) we used the same configuration but two different gratings H1200R and H1200B, for the red and blue spectral regions respectively. Using the same configuration a reciprocal dispersion of 0.39 Å was obtained which yields a spectral resolution of 0.94 Å and a useful wavelength range of 385 Å centered at 6563 Å (Hα), 5876 Å (HeI D_3), 4861 Å (Hβ), 3950 Å (Ca II H&K) respectively.

In Table 1 we give the observing log. For each spectral region observed we list the date, UT, orbital phase (φ) and signal to noise ratio (S/N) obtained.

We also analyse here echelle spectra obtained with the 4.2 m William Herschel Telescope (WHT) and the Utrecht Echelle Spectrograph (UES) on July 31 1993 that we have retrieved from La Palma Data Archive (Zuiderwijk et al. 1994). These WHT/UES spectra were obtained with echelle 31 (31.6 grooves per mm) and a 1280 x 1180 pixel EEV6 CCD as detector. The central wavelength is 6127 Å and covers a wavelength range from 4845 to 8805 Å over 53 echelle orders. The achieved reciprocal dispersion ranges from 0.045 to 0.080 Å/pixel. In order to improve the S/N ratio and to avoid cosmic ray events, the final spectrum analysed here is the resulting from combine 28 CCD images with exposure times of 240 s each, obtaining a final spectrum with a S/N of 315 in the Hα line region. In Table 2 we give the wavelength range and the spectral lines of interest in each echelle order.

In addition we also use one spectrum in the region of the Ca II IRT lines taken on January 16 1997 with the 1.0 m Jacobus Kapteyn Telescope (JKT) using the Richardson-Brealey Spectrograph (RBS) with a grating of 1200 grooves per mm, and a 1024 x 1024 pixel TEK4 CCD as detector. The reciprocal dispersion achieved is 0.85 Å/pixel which yields a spectral resolution of 1.7 Å and a useful wavelength range of 865 Å centered at 8765 Å.

The spectra have been extracted using the standard reduction procedures in the IRAF [1] package (bias subtraction, flat-field division, and optimal extraction of the spectra). The reduction of the JKT/RBS spectrum was carried out using the reduction package $\mathrm{R_E D^{uc}_m E}$ (Cardiel & Gorgas 1997, see also http://www.ucm.es/OTROS/Astrof/reduceme/reduceme.html). The wavelength calibration was obtained by taking spectra of a Cu-Ar lamp in the INT/IDS spectra, a Th-Ar lamp in the WHT/UES spectrum and a Cu-Ne lamp in the JKT/RBS spectrum. Finally, the spectra have been normalized by a polynomial fit to the observed continuum.

3. Stellar parameters of the binary system EZ Peg

EZ Peg is a double-lined spectroscopic binary with an orbital period of 11.6598 days (Griffin 1985), classified as G5V-IV/K0IV. It is in synchronous rotation with a photometric period of 11.6626 days (Howell et al. 1986). In Table 3 we show the

[1] IRAF is distributed by the National Optical Observatory, which is operated by the Association of Universities for Research in Astronomy, Inc., under contract with the National Science Foundation.

Table 2. UES spectral orders

No.	λ_i	λ_f	Chromospheric Lines	Other lines
1	4845.80	4897.29	Hβ	
2	4887.53	4939.46		
3	4929.98	4982.35		
4	4973.16	5026.00		
5	5017.11	5070.41		
6	5061.85	5115.62		
7	5107.38	5161.63		
8	5153.74	5208.48	Mg i b λ5167-72-83	
9	5200.94	5256.19		
10	5249.02	5304.77		
11	5297.99	5354.27		
12	5347.89	5404.69		Ti i λ5366
13	5398.73	5456.07		Ti i λ5426
14	5450.54	5508.43		
15	5503.36	5561.81		
16	5557.21	5616.23		
17	5612.13	5671.73		
18	5668.14	5728.34		
19	5725.28	5786.09		
20	5783.58	5845.01		
21	5843.08	5905.14	Na i D_1, D_2, He i D_3	Ti i λ5866
22	5903.82	5966.53		
23	5965.84	6029.20		
24	6029.17	6093.21		
25	6093.87	6158.59		
26	6159.96	6225.39		
27	6227.51	6293.66		
28	6296.55	6363.44		
29	6367.15	6434.78		Fe i λ6411.66
30	6439.35	6507.75		Fe i λ6495
31	6513.20	6582.39	Hα	
32	6588.77	6658.76		
33	6666.11	6736.93		Fe i λ6678
”				Li i λ6708
”				Ca i λ6718
34	6745.30	6816.95		
35	6826.39	6899.90		O_2 λ6867
36	6909.45	6982.85		
37	6994.56	7068.87		
38	7081.80	7157.03		
39	7171.24	7247.43		
40	7262.98	7340.14		
41	7357.09	7435.25		
42	7453.68	7532.86		
43	7552.84	7633.08		B-band λ7600
44	7654.68	7736.00		K i λ7665, 7699
45	7759.30	7841.73		
46	7866.82	7950.40		
47	7977.38	8062.12		
48	8091.08	8177.03		
49	8208.08	8295.27		
50	8328.51	8416.99		Ti i (M.33)
51	8452.54	8542.33	Ca ii IRT λ8498, 8542	Ti i λ8468
”				Fe i λ8514
”				Ti i λ8518
52	8580.32	8671.46	Ca ii IRT λ8662	Fe i λ8621
53	8712.02	8804.56		

adopted stellar parameters from Strassmeier et al. (1993) except for T_{conj} (see below).

3.1. Radial velocities

In our high resolution echelle spectrum we can resolve both components in all the orders. We have calculated the radial velocity difference for this observation using 39 lines clearly seen in the echelle spectrum as double lines. The value obtained is 16.17 ± 0.72 km s^{-1} which results in a value for the orbital phase of 0.944 ± 0.002.

According to the ephemeris given by Strassmeier et al. (1993) the calculated phase for this spectrum is 0.997, which is clearly in disagreement with our observation, since at this phase the radial velocity difference is 0.92 km s^{-1} which yields a difference in wavelength between both components of only 0.02 Å. This $\Delta\lambda$ is lower than the resolution of the spectrum and then the lines from both components should be blended. Similar problems have been found in the other spectra when we use this ephemeris. The phase deviation is the same for all the observations and is very large to be ascribed to orbital period variations, so we thought of an error in the heliocentric Julian date on conjunction (T_{conj}). In effect, we have found a mistake in the T_{conj} given in the Strassmeier et al. (1993) catalog where the orbital data by Griffin (1985) are compiled. In the original paper the epoch is determined using Modified Julian Date (MJD) and so a difference of 0.5 days must be added to the Strassmeier et al. (1993) date which used 2440000.0 Julian day as reference date. The orbital phase of the echelle spectrum obtained using the corrected value of T_{conj} (2445737.165) is 0.954. Now, the difference with the orbital phase that we deduce from our spectrum is only 0.01, which is within the uncertainties given by Griffin (1985). We would notice that the large discrepancies in the radial velocities which Gunn et al. (1996) found could be reduced using the corrected T_{conj}. Therefore we have used the corrected T_{conj} given in Table 3 to calculate the orbital phases of all the observations reported in this paper.

3.2. Spectral type and luminosity class

Several Ti I lines can be used as a luminosity classification criterium (Keenan & Hynek 1945; Kirkpatrick et al. 1991; Ginestet et al. 1994; Jashek & Jashek 1995) because they present a positive luminosity effect (i.e. they are stronger in giants than in dwarfs). We have analysed the behaviour of the Ti I lines that appear in our echelle spectrum in order to improve the luminosity classification of the EZ Peg components.

In Fig. 1 we can notice the enhancement of the multiplet 33 Ti I lines for the system in comparison with main sequence stars of spectral type similar to the components of EZ Peg. It is worth mentioning the case of the Ti I λ8382 line which is even more intense than the Fe I λ8388 line, showing a behaviour different from that in the subgiant reference star (see Fig. 1 lower panel). This behaviour can be also observed in other Ti I lines like λ5366.651 (Multiplet 35), λ5446.593 (M. 3), λ5866.453, λ5937.806 and λ5941.755 (M. 72), λ6554.226 and λ6556.066

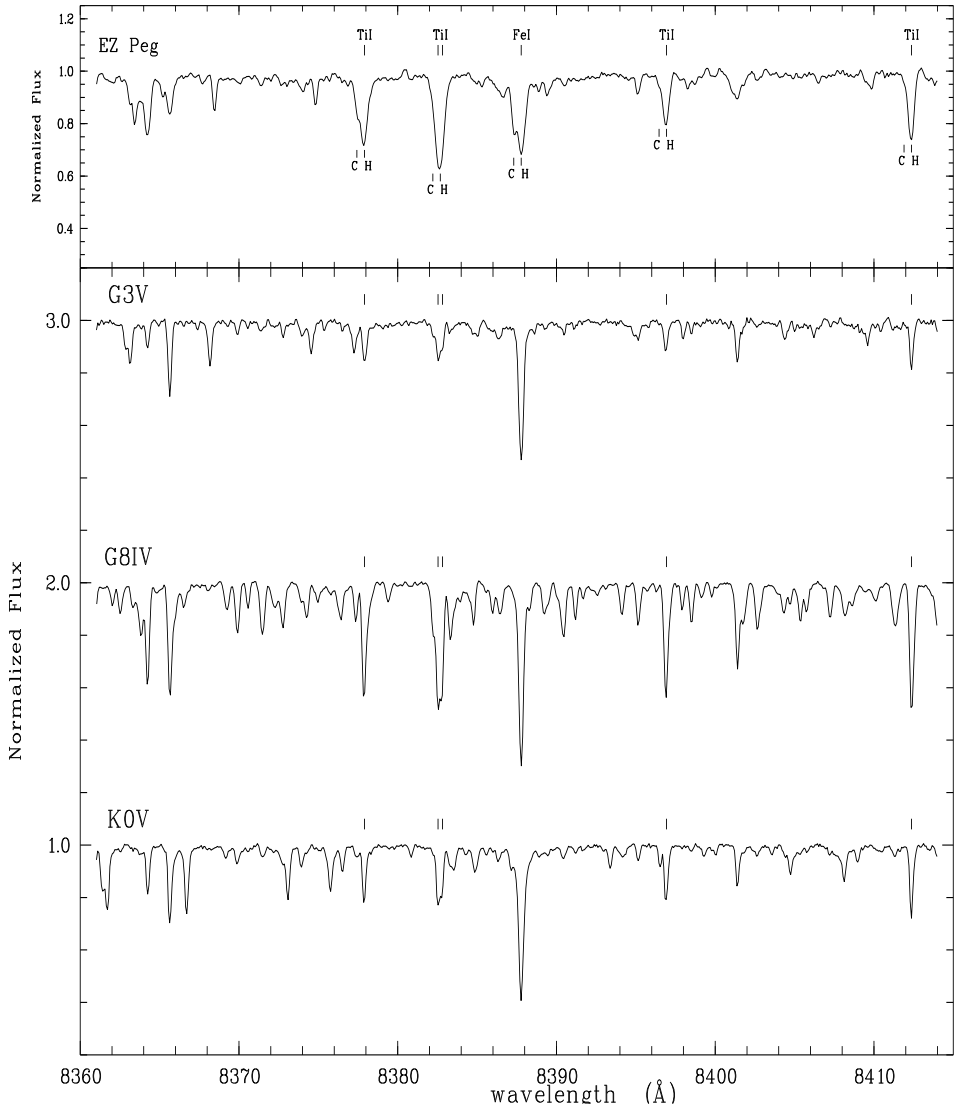

Fig. 1. WHT/UES (Jul 1993), spectra in the region of several lines of Ti I (M.33). In the upper panel we plot EZ Peg and in the lower panel three reference stars: HD 186427 (G3V), HD 44867 (G8IV), HD 185144 (K0V).

Table 3. Stellar parameters

T_{sp}	SB	R ($R_\odot$)	d (pc)	B-V	V-R	T_{conj} (H.J.D.)	P_{orb} (days)	P_{rot} (days)	Vsin*i* (km s^{-1})
G5V-IV/K0IV:	2	-	83	0.73/0.91	0.58/0.71	2445737.165	11.6598	11.6626	9/7

(M.102), λ6599.112 (M.19). These results suggest a clear difference in luminosity class between the two components of the system, being the G5 primary star more evolved than a subgiant, meanwhile the K0 star is probably a luminosity class V star.

As is explained in the following section all the activity indicators analysed here show that the hot component is the active star of the system, contrary to the usual behaviour observed in chromospherically active binaries. Only in some BY Dra stars the hot component tends to be the most active star of the system or even the only active component (Montes et al. 1996a). So we have used our Ca II K spectra to determine the absolute visual magnitude, M_V of the active component by the application of the Wilson-Bappu effect (Wilson & Bappu 1957). The mean emission line width measured in our Ca II K spectra is 1.229 Å, which come out to 60.39 km s^{-1} after the quadratic correction of the instrumental profile. We have used the relation found for chromospherically active binaries by Montes et al. (1994) obtaining M_V = 2.27. This value is lower than the M_V that corresponds to a G5V ($M_V(T_{sp})$ = 5.1 from Landolt-Börnstein (Schmidt-Kaler 1982)) but higher than for a G5III ($M_V(T_{sp})$ = 0.9). This result indicates that the active component of EZ Peg may be of luminosity class IV or higher.

Table 4. Hα line measures in the observed and subtracted spectrum

Obs.	φ	Observed Hα Spectrum			Subtracted Hα Spectrum			
		W_{obs} (Å)	R_c	F(1.7Å)	W_{sub} (Å)	I	EW (Å)	log F_S
UES 1993	0.954	0.96	1.325	1.987	1.62	0.882	2.085	7.06
INT 1995	0.416	0.65	1.139	1.695	1.70	0.655	1.488	6.91
”	0.501	0.54	1.059	1.657	1.69	0.639	1.400	6.89
INT 1996	0.141	1.48	1.131	1.779	2.43	0.604	2.272	7.10
”	0.224	1.55	1.157	1.812	2.30	0.634	1.862	7.01
”	0.306	1.35	1.134	1.784	2.16	0.638	1.677	6.96

The difference in luminosity class between the hot and cool components that our spectra indicate could explain why the hot component is the active star (see below), since if the hot component is a more evolved star it could have developed a deep convective zone and therefore, according to the dynamo mechanism, should present a higher activity level. Anyway the cooler K0V component could also be active and present a faint emission in the H & K lines, but due to the small contribution of that star to the combined spectrum of the system, this emission is very difficult to be observed.

3.3. The Li I λ6707.8 line

We also analyse here the Lithium abundance of EZ Peg using the Li I λ6707.8 line. This line appears in the order 33 of the WHT/UES echelle spectrum together with the Fe I λ6678 and Ca I λ6718 lines. In Fig. 2 we can clearly see the Fe I and Ca I lines from both components, the expected positions of these features for the hot (H) and cool (C) are given in this figure. However, the absorption Li I line appears centered in the wavelength-position corresponding to the hot component, so we can suppose that the absorption line comes only from this star or that the contribution of the cool component to the observed Li I is very small. This assumption seems to be reasonable because, as we show below, the hot component is the active star of the system and a high Li I abundance is found in chromospherically active binaries (Fernández-Figueroa et al. 1993; Barrado et al. 1997). In order to obtain the Li I equivalent width (EW), we have corrected the total EW measured, EW(Li I+Fe I)=50.4 (mÅ) from the relative contribution to the continuum (0.65). Then the contribution from the blend with the Fe I λ 6704.41 line must be subtracted. The EW of the Fe I line was calculated from the empirical relationship with (B-V) given by Soderblom et al. (1990), obtaining EW(Fe I)=15.8 (mÅ), the same value is found with the relationship given by Favata et al. (1993) using the effective temperature. Finally, the corrected $EW(Li\ I)_{corr}$=61.7 (mÅ) was converted into abundances by means of the curves of growth computed by Pallavicini et al. (1987), obtaining log N(Li I)=2.15 (on a scale where log N(H)=12.0) with an accuracy of $\approx$ 0.30 dex. This high Li I abundance is similar to that obtained for other chromospherically active binaries by Fernández-Figueroa et al. (1993) and Barrado et al. (1997) and it is related to the high activity level of EZ Peg.

4. Chromospheric activity indicators

In the following we describe the behaviour of the different optical chromospheric activity indicators (formed at different atmospheric heights) observed for EZ Peg: Na I D_1, D_2, and Mg I b triplet (upper photosphere and lower chromosphere), Ca II IRT lines (lower chromosphere), Hα, Hβ, Ca II H & K (middle chromosphere), and He I D_3 (upper chromosphere). The chromospheric contribution in these features has been determined using the spectral subtraction technique described in detail by Montes et al. (1995a, b, c), (see also Paper I). The synthesized spectrum has been constructed with reference stars of spectral types G5V and K0IV, taken from the spectral library of Montes et al. (1997a), in the case of the INT/IDS spectra. For the WHT/UES spectrum we have used a G3V and K0V taken during the same observing run, and for the JKT/RBS spectrum a G5III-IV and K0V have been used. The use of reference spectra of spectral type slightly different for each observing run and different also from the system component spectra introduce some residual in the absorption lines, but it does not affect significantly the excess emission equivalent width measures in the subtracted spectra. The uncertainties are within similar order to that obtained in the reduction, synthesis and fitting procedures. Furthermore, we have considered a clear detection of excess emission or absorption lines only when these features in the difference spectrum are larger than 3 σ.

The contribution of the hot and cool components to the total continuum that yields a better fit between the observed and subtracted spectra is 0.65/0.35.

The line profiles are displayed in Figs. 1 - 8. For each spectrum we plot the observed (solid-line), the synthesized (dashed-line) and the subtracted one, additively offset for better display (dotted line).

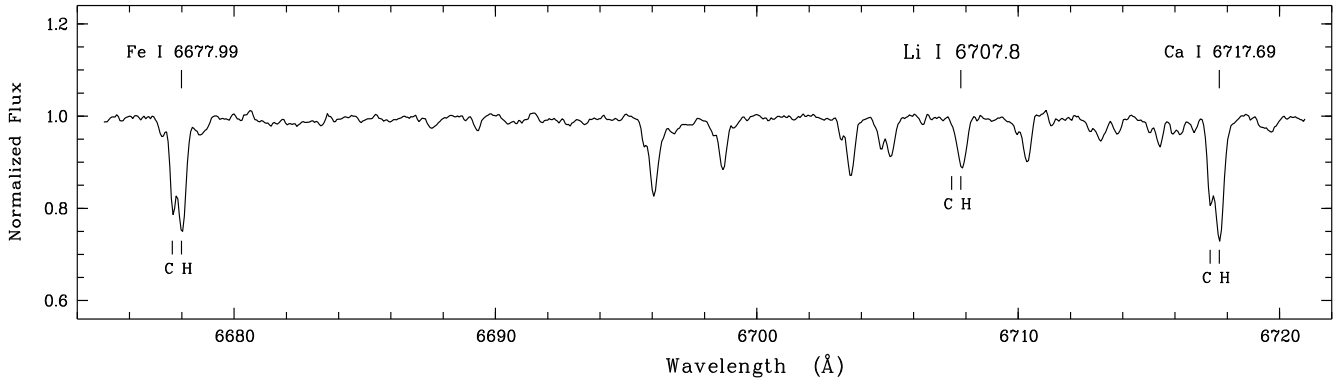

Fig. 2. WHT/UES (Jul 1993), spectrum in the region of the Li I 6707.8 Å line including also the Fe I 6677.99 Å and Ca I 6717.69 Å . The expected positions of this features for the hot (H) and cool (C) components are given.

Table 5. Parameters of the broad and narrow Gaussian components used in the fit of the Hα subtracted spectra

		Hα broad component				Hα narrow component			
Obs.	φ	I	FWHM (Å)	EW_B (Å)	EW_B/EW_T (%)	I	FWHM (Å)	EW_N (Å)	EW_N/EW_T (%)
UES 1993	0.954	0.273	3.935	1.143	54.8	0.648	1.367	0.942	45.2
INT 1995	0.416	0.152	4.035	0.651	43.7	0.535	1.470	0.837	56.3
”	0.501	0.129	4.096	0.562	40.1	0.535	1.470	0.838	59.9
INT 1996	0.141	0.123	9.418	1.209	53.2	0.493	2.028	1.064	46.8
”	0.224	0.124	5.622	0.740	39.7	0.520	2.028	1.122	60.3
”	0.306	0.091	5.528	0.536	32.0	0.572	1.876	1.142	68.0

4.1. The Hα line

We have taken several spectra of EZ Peg in the Hα line region in three different epochs. One WHT/UES spectrum in July 1993 at the orbital phase 0.954 (Fig. 3), two INT/IDS spectra in September 1995 at the phases 0.416 and 0.501 (Fig. 4) and three more INT/IDS spectra in November 1996 at the phases 0.141, 0.224 and 0.306 (Fig. 5). In all the spectra we can see the Hα line in emission above the continuum with an asymmetry in the wavelength position corresponding to the Hα absorption line of the cool component. The spectral subtraction reveals that the hot star is responsible for the excess Hα emission.

Table 4 gives the Hα line parameters, measured in the observed and subtracted spectra of EZ Peg as follows: column (1) the observing run, column (2) the orbital phase (φ) and columns (3), (4), (5) the following parameters measured in the observed spectrum: the full width at half maximum (W_{obs}); the residual intensity, R_c; and the Hα core flux, F(1.7Å), measured as the residual area below the central 1.7 Å passband. The last four columns give the following parameters measured in the subtracted spectrum: the full width at half maximum (W_{sub}), the peak emission intensity (I), the excess Hα emission equivalent width (EW(Hα)), and absolute fluxes at the stellar surface $\log F_S$(Hα) obtained with the calibration of Pasquini & Pallavicini (1991) as a function of (V - R), very similar values of F_S(Hα) are obtained using the more recent calibration of Hall (1996) as a function of (V - R) and (B - V). As can be seen in Table 4 and Figs. 3, 4 and 5 the excess Hα emission of EZ Peg show small variations with the orbital phase and also seasonal variations from Jul 93 to Nov 96. The higher Hα EW has been reached in the first night of the 1996 run and in the 1993 observation. The higher values correspond to the orbital phases closer to the conjunction (0.0).

The Hα subtracted profiles present at all the epochs broad wings which are not well matched using a single-Gaussian fit. These profiles have therefore been fitted using two Gaussian components. The parameters of the broad and narrow components used in the two-Gaussian fit are given in table 5 and the corresponding profiles are plotted in the left panel of Figs. 3, 4 and 5. In some cases the blue wing is noticeable stronger than the red wing and the fit is better matched when the broad component is blue-shifted with respect to the narrow component. The cool component of EZ Peg cannot account for this effect since any emission from that star would be on the red side of the observed line for these orbital phases. We have also observed broad components in the most active systems of the sample of Paper I which we interpreted as microflaring that occurs in the chromosphere by similarity with the broad components also found in the chromospheric Mg II h & k lines (Wood et al. 1996) and in several transition region lines of active stars (Linsky & Wood

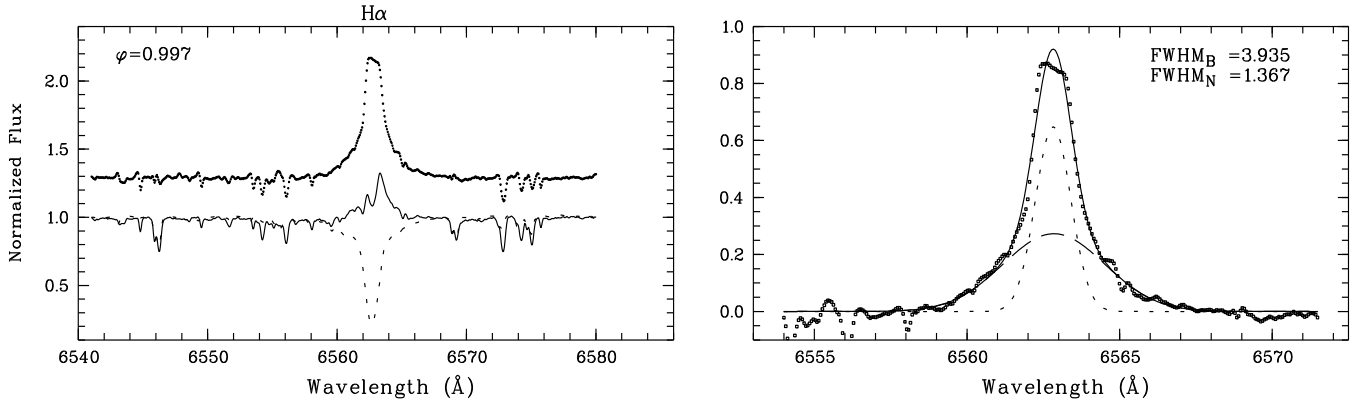

Fig. 3. WHT/UES Hα spectrum (Jul 1993). In the left panel we plot the observed spectrum (solid-line), the synthesized spectrum (dashed-line), the subtracted spectrum, additively offset for better display (dotted line). In the right panel we plot the subtracted Hα profile (dotted line). and the the two Gaussian components fit (solid-line). The sort-dashed-line represents the broad component and the large-dashed-line the narrow one.

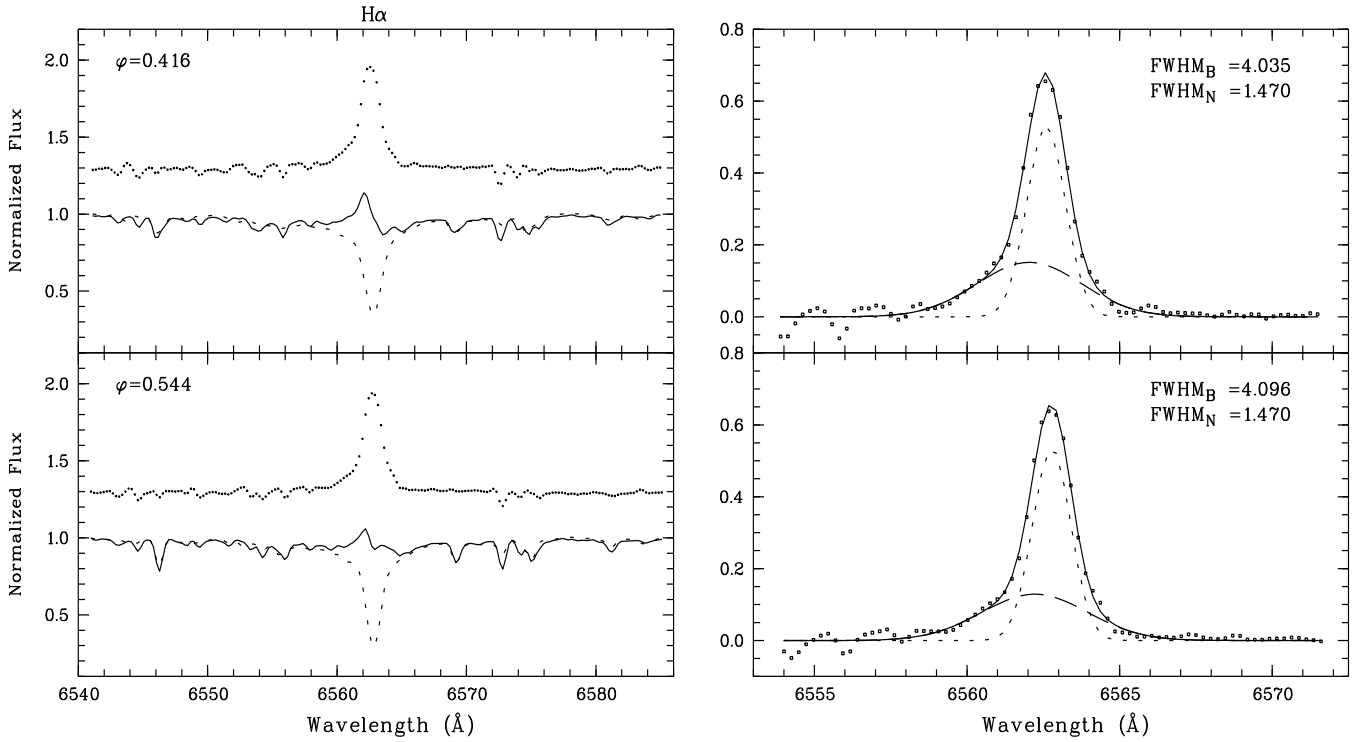

Fig. 4. INT/IDS Hα spectra (Sep 1995), as in Fig. 3

1994; Linsky et al. 1995; Wood et al. 1996, 1997; Dempsey et al. 1996a, b; Robinson et al. 1996). The contribution of the broad component to the total EW of the line of EZ Peg ranges between 32% and 55% which is in the range observed to the stars analysed in Paper I. The larger changes in the excess Hα emission appear to occur predominantly in the broad component and its contribution is related to the degree of stellar activity. It is noticeable the change in the wings of the Hα line from the 1st to the 2nd night of the 1996 run, the two Gaussian components fit reveals that the contribution of the broad component changes from 53.2% to 39.7% (see Fig. 5).

4.2. The Hβ line

Two spectra in the Hβ line region are available. The WHT/UES spectrum (July 1993) and other in the INT/IDS 1996 run. In both spectra the Hβ line appears in absorption and the application of the spectral subtraction technique reveals a clear excess emission in this line (see Fig. 6). Again the relative velocity shift shows that the emissions belong to the hotter component. Contrary to the case of the Hα line the Hβ subtracted profiles do not present broad wings and they are well matched using a single-Gaussian fit.

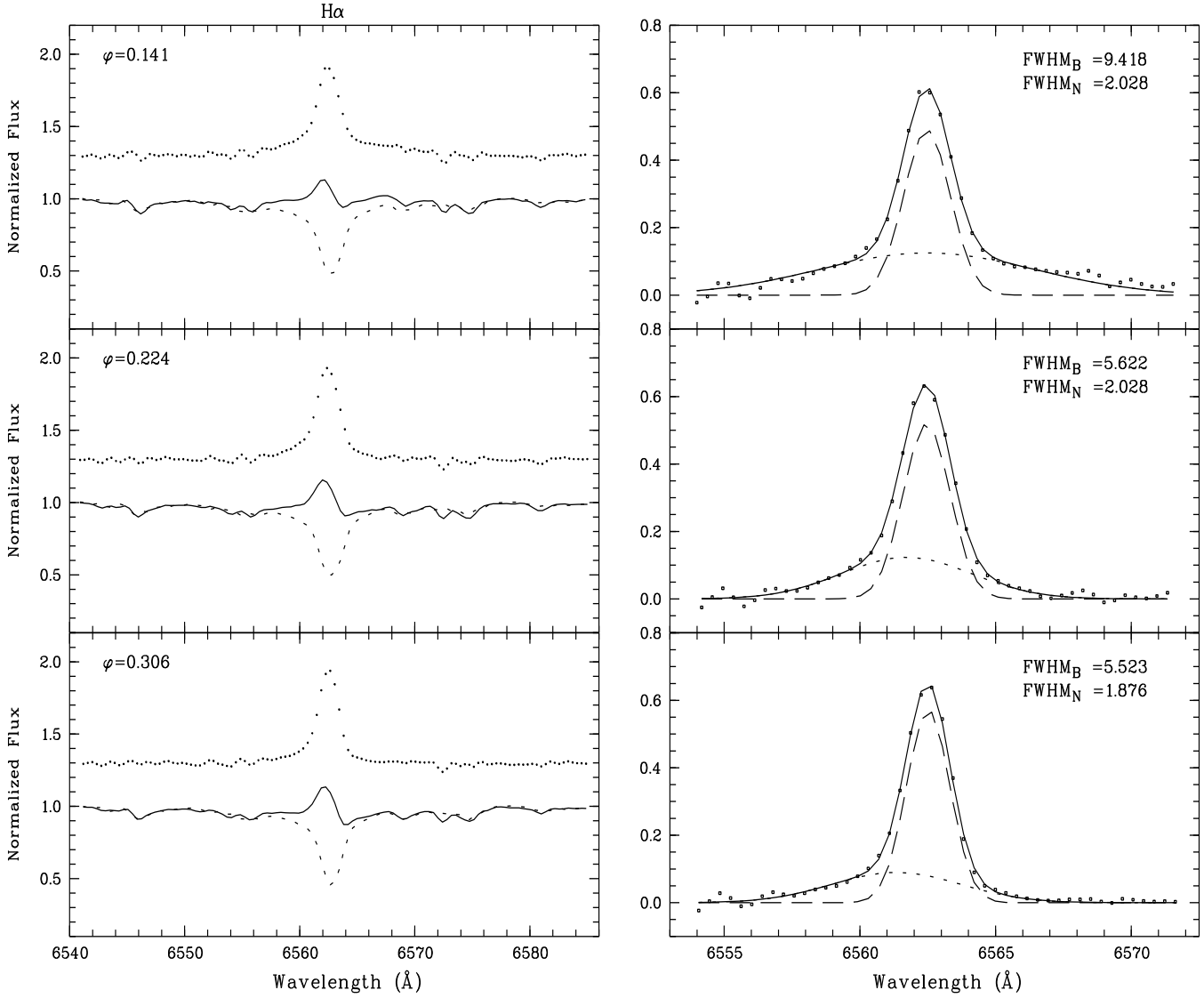

Fig. 5. INT/IDS Hα spectra (Nov 1996), as in Fig. 3

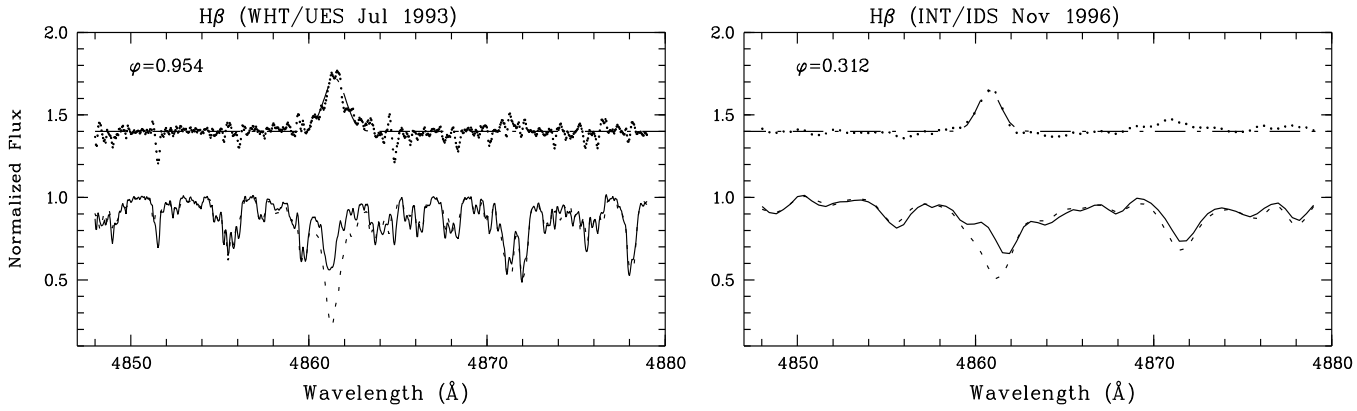

Fig. 6. WHT/UES Hβ (Jul 1993) and INT/IDS Hβ (Nov 1996) spectra. For each spectrum we plot the observed spectrum (solid-line), the synthesized spectrum (dashed-line), the subtracted spectrum, additively offset for better display (dotted line). and the Gaussian fit to the subtracted spectrum (dotted-dashed line)

Table 6 gives the Hβ line parameters, measured in the observed and subtracted spectra as in the case of the Hα line, see also our previous study of the excess Hβ emission in active binaries (Montes et al. 1995d).

In Table 6 we also give the ratio of excess emission EW, $\frac{\mathrm{EW(H}\alpha)}{\mathrm{EW(H}\beta)}$, for the two H$\beta$ observations of EZ Peg, and the ratio of excess emission $\frac{\mathrm{E_{H}}\alpha}{\mathrm{E_{H}}\beta}$ with the correction:

$$\frac{\mathrm{E_{H}}\alpha}{\mathrm{E_{H}}\beta} = \frac{\mathrm{EW(H}\alpha)}{\mathrm{EW(H}\beta)} * 0.2444 * 2.512^{(B-R)}.$$

given by Hall & Ramsey (1992) that takes into account the absolute flux density in these lines and the color difference in the components.

We have used this ratio as a diagnostic for discriminating between the presence of plages and prominences in the stellar surface, following the results of Hall & Ramsey (1992) who found that low $\mathrm{E_{H}}\alpha/\mathrm{E_{H}}\beta$ ($\approx$ 1-2) can be achieved both in plages and prominences viewed against the disk, but that high ratios ($\approx$ 3-15) can only be achieved in extended regions viewed off the limb. The high ratio ($\mathrm{E_{H}}\alpha/\mathrm{E_{H}}\beta > 3$, see Table 6) that we have found in EZ Peg indicates that the emission would arise from extended regions (prominences).

The excess Hβ emission is somewhat larger in the 1993 observation than in the last night observation of the 1996 run, in agreement with the behaviour observed for the Hα line.

4.3. The Na I D_1 and D_2 and He I D_3 lines

We have five spectra of EZ Peg in the region of Na I D_1 and D_2 and He I D_3 lines: one WHT/UES spectrum in July 1993 at the orbital phase 0.954 (Fig. 7), two INT/IDS spectra in September 1995 at the phases 0.414 and 0.500 and two spectra in INT/IDS November 1996 at the phases 0.225 and 0.310 (Fig. 8). We have not detected any significant absorption or emission for He I D_3.

Saar et al. (1997) in their study of He I D_3 in G and K dwarfs found that while for few active stars the He I D_3 line behaves "normally", increasing in absorption with increasing rotation, and showing consistent correlations with other activity indicators, the behavior clearly diverges when stars become very active. They found a large filling-in He I D_3 line in some very active K stars. On the other hand, they also found He I D_3 EW significantly lower than the theoretical maximum value given by Andretta & Giampapa (1995), suggesting that the line could be filling-in due to frequent low-level flaring.

Both facts could explain the absence of emission or absorption due to a total filling-in of the He I D_3 line that we have found in EZ Peg and also in other dwarfs and subgiants chromospherically active binaries (see Paper I), since these stars are very active and also present low-level flaring (microflares) as indicated by the Hα broad component that we have found (see sect. 4.1 and Paper I). In some cases He I D_3 goes into emission due to flares (Huenemoerder & Ramsey 1987; Huenemoerder et al. 1990; Montes et al. 1996b; Paper I). However, in the most evolved stars the behaviour is different as consequence of the lower chromospheric densities of these stars, as it is suggested by Saar et al. (1997) and as it is indicated by the presence of the He I D_3 in absorption that we have reported in Paper I for several chromospherically active binaries with giant components.

In the Na I D_1 and D_2 lines the spectra are too noisy to distinguish a clear filled-in. Once again we can observe (see Fig. 7) that the redward lines of the double-lined spectrum usually are the deepest, but in the Na I D blueshifted components are the deepest ones. As it is well known, the Na I D lines are very sensitive to the temperature; this behaviour of the lines confirms that the hot star of the system is the redshifted one, which, as mentioned above, shows very high activity in Hα.

4.4. The Mg I b triplet lines

The Mg I b triplet lines λ5167.33, λ5172.68, and λ5183.61 are formed in the lower chromosphere and the region of temperature minimum and they are good diagnostics of photospheric activity (Basri et al. 1989). A small filling-in of these lines have been recently found in some RS CVn system (Gunn & Doyle 1997; Gunn et al. 1997). As in the case of the Na I D_1 and D_2 lines, in the subtracted spectrum corresponding to the echelle images no clear filled-in has been found. Thus the photospheric activity in EZ Peg is very low.

4.5. The Ca II H & K and Hϵ lines

We have taken three spectra in the Ca II H & K line region during the 1996 run (see Fig. 9). These spectra exhibit strong Ca II H & K emission lines and a small bump in the wavelength-position corresponding to the Hϵ line. The H & K emission lines appear blue-shifted with respect to the observed absorption lines in agreement with the orbital phase, which confirms that the emission originates in the hot component. The spectral subtraction yields a satisfactory fit and reveals a small but clear emission in the Hϵ line.

The excess Ca II H & K and Hϵ emissions equivalent widths (EW) have been measured by reconstruction of the absorption line profile (described by Fernández-Figueroa et al. 1994) and using the spectral subtraction technique (explained by Montes et al. 1995c, 1996a). The Ca II H & K surface flux, $\mathrm{F_S}$(Ca II H & K) has been obtained by means of the linear relationship between the absolute surface flux at 3950 Å (in erg $\mathrm{cm^{-2}\ s^{-1}\ Å^{-1}}$) and the colour index (V-R) by Pasquini et al. (1988).

Table 7 gives the Ca II H & K and Hϵ line parameters, measured in the observed and subtracted spectra. Column (1) gives the observing run. Column (2) gives the orbital phase (φ). In columns (3) and (4) we list the EW for the K and H lines, obtained by reconstruction of the absorption line profile, in columns (5) to (7) we give the EW for the K, H and Hϵ lines, measured in the subtracted spectrum, and in columns (8) to (10) the corresponding surface fluxes are listed.

The excess Ca II H & K and Hϵ emissions change with the orbital phase during the three nights of the 1996 run in the same way as the corresponding excess Hα emissions.

Table 6. Hβ line measurements in the observed and subtracted spectrum

Obs.	φ	Observed Hβ Spectrum			Subtracted Hβ Spectrum			$\frac{EW(H\alpha)}{EW(H\beta)}$	$\frac{E_{H\alpha}}{E_{H\beta}}$
		W_{obs} (Å)	R_c	F(1.7Å)	W_{sub} (Å)	I	EW (Å)		
UES 1993	0.954	0.91	0.561	1.235	0.94	0.364	0.489	4.27	3.49
INT 1996	0.312	2.13	0.660	1.237	1.54	0.244	0.411	4.08	3.33

Table 7. Ca II H & K and Hϵ lines measures in the observed and subtracted spectrum

Obs.	φ	Reconstruction		Spectral subtraction			Absolute flux		
		EW (K)	EW (H)	EW (K)	EW (H)	EW (Hϵ)	log F (K)	log F (H)	log F (Hϵ)
INT 1996	0.148	0.982	0.718	1.246	0.931	0.292	6.91	6.79	6.28
"	0.220	0.975	0.671	1.191	0.910	0.194	6.82	6.78	6.10
"	0.314	0.948	0.628	1.142	0.907	0.185	6.87	6.77	6.08

Table 8. Ca II IRT lines measured in the observed and subtracted spectra

Obs.	φ	Reconstruction			Spectral subtraction			Absolute flux		
		EW λ8498	EW λ8542	EW λ8662	EW λ8498	EW λ8542	EW λ8662	log F λ8498	log F λ8542	log F λ8662
UES 1993	0.954	0.256	-	0.238	0.680	-	0.892	6.43	-	6.55
JKT 1997	0.511	-	-	-	0.397	0.471	0.453	6.19	6.26	6.25

4.6. The Ca II IRT lines

The Ca II infrared triplet (IRT) λ8498, λ8542, and λ8662 lines are other important chromospheric activity indicators (Linsky et al. 1979; Foing et al 1989; Dempsey et al. 1993). These lines share the upper levels of the Ca II H & K transitions (see for example Mihalas 1978), but unlike the blue Ca II lines, the IRT lies in a region of the spectrum with a well-defined continuum, making the calibration simpler. The IRT is formed in the lower chromosphere. Shine & Linsky (1972, 1974) observed solar IRT plage profiles concluding that the emission results from a steepening of the temperature gradient in the chromosphere. This forces the temperature, electron density, and Ca II density population to be higher for a given optical depth, compared to the quiet chromosphere, thus increasing the source function thereby producing emission in the line cores.

In the observations carried out by Dempsey et al. (1993) only one star of the sample (BY Dra) showed emission above the local continuum in only the λ8498 line, and other seven stars revealed emission rising above the shallow line core.

The λ8498 and λ8662 lines are included in the 1993 WHT/UES echelle spectrum of EZ Peg (see Fig. 10), and both lines exhibit a strong emission superposed to the red wing of the corresponding absorption line, in agreement with the orbital phase (0.954). In the 1997 JKT/RBS spectrum at orbital phase 0.511 the three Ca II IRT lines are included (see Fig. 11). In this case the lines show a small emission reversal centered at the absorption line in the observed spectrum and a clear excess emission in the difference spectrum.

Table 8 gives the Ca II IRT line parameters, measured in the observed spectra by reconstruction of the absorption line profile, and using the spectral subtraction. The columns in this table have the same meaning as for the Ca II H & K lines (see Table 7). Notice that the underestimation of the reconstruction method is larger for the IRT lines than for the Ca II H & K lines. The absolute fluxes at the stellar surface have been obtained using the calibration of Hall (1996) as a function of (V - R).

As in the case of the Hα line the subtracted profiles of the λ8498 and λ8662 lines also present broad wings. Therefore we have used, as for the Hα profile, a two gaussian (broad and narrow) fit. In Table 9 we list the parameters (I, FWHM, EW) of the broad and narrow components. The narrow components of both lines are very similar; however, the contribution of the

Table 9. Parameters of the broad and narrow Gaussian components used in the fit of the Ca II IRT subtracted spectra

Obs.	φ	Broad component				Narrow component			
		I	FWHM (Å)	EW_B (Å)	EW_B/EW_T (%)	I	FWHM (Å)	EW_N (Å)	EW_N/EW_T (%)
Ca ii IRT line λ8498									
UES 1993	0.954	0.089	2.497	0.237	34.8	0.693	0.600	0.442	65.2
Ca ii IRT line λ8662									
UES 1993	0.954	0.086	5.393	0.452	50.7	0.564	0.733	0.440	49.3

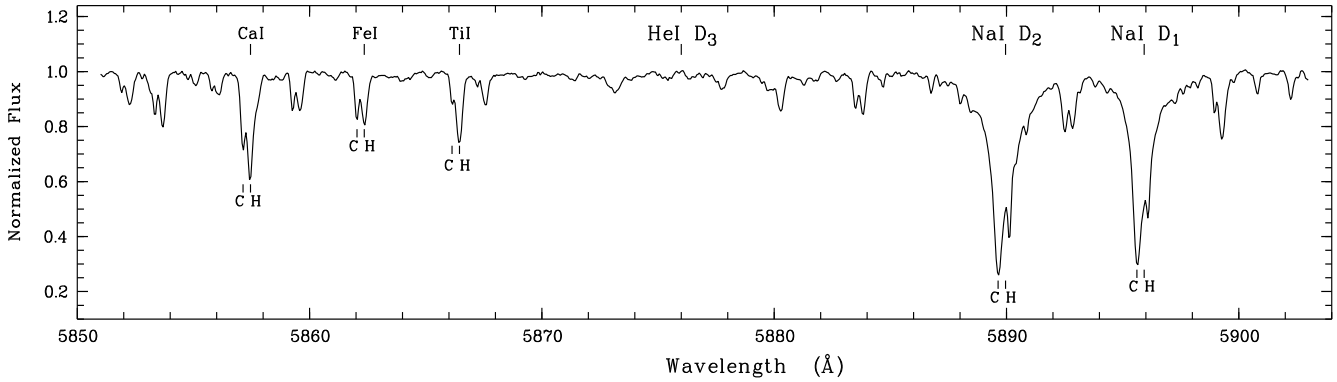

Fig. 7. WHT/UES (Jul 1993), spectrum in the region of the NaI and HeI lines including also the CaI 5857.454 Å, FeI 5862.357 Å and TiI 5866.453Å. The expected positions of these features for the hot (H) and cool (C) components are given.

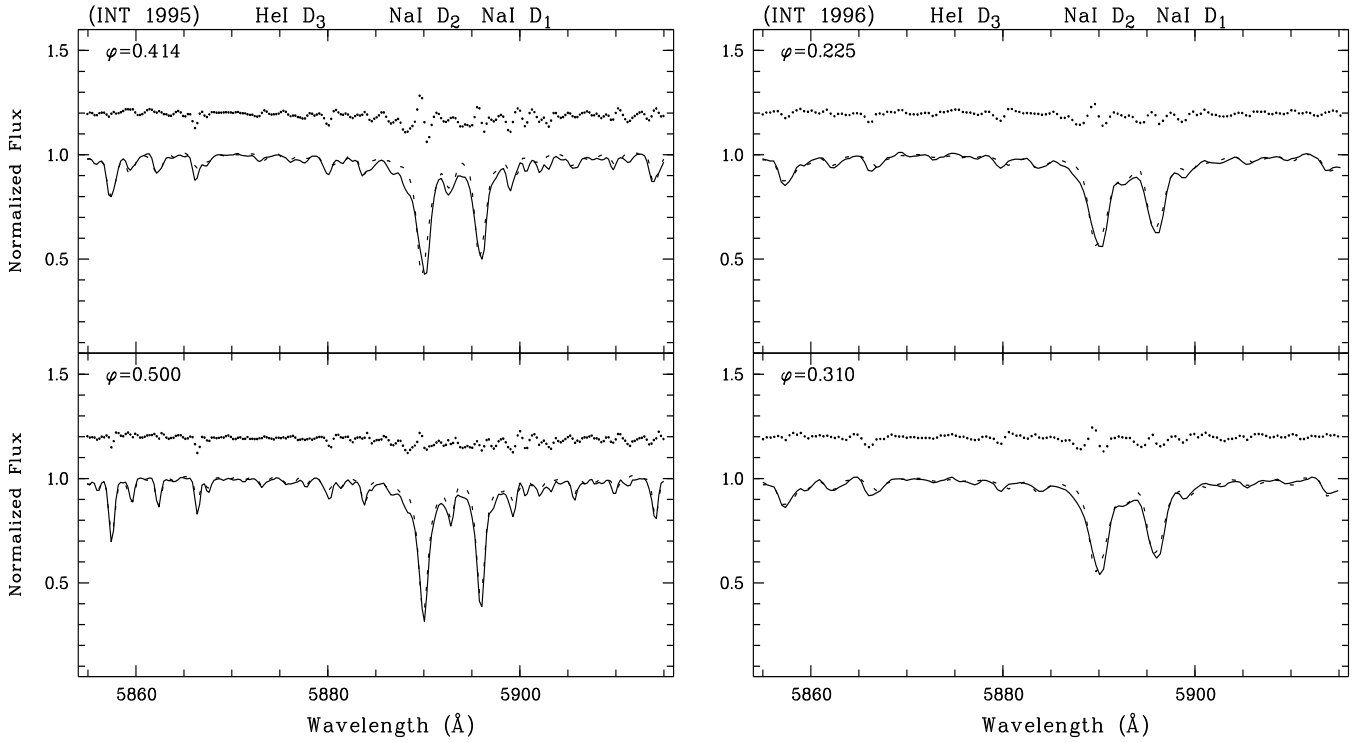

Fig. 8. INT/IDS spectra in the region of the NaI and HeI lines (Sep 1995) and (Nov 1996). For each spectrum we plot the observed spectrum (solid-line), the synthesized spectrum (dashed-line), the subtracted spectrum, additively offset for better display (dotted line).

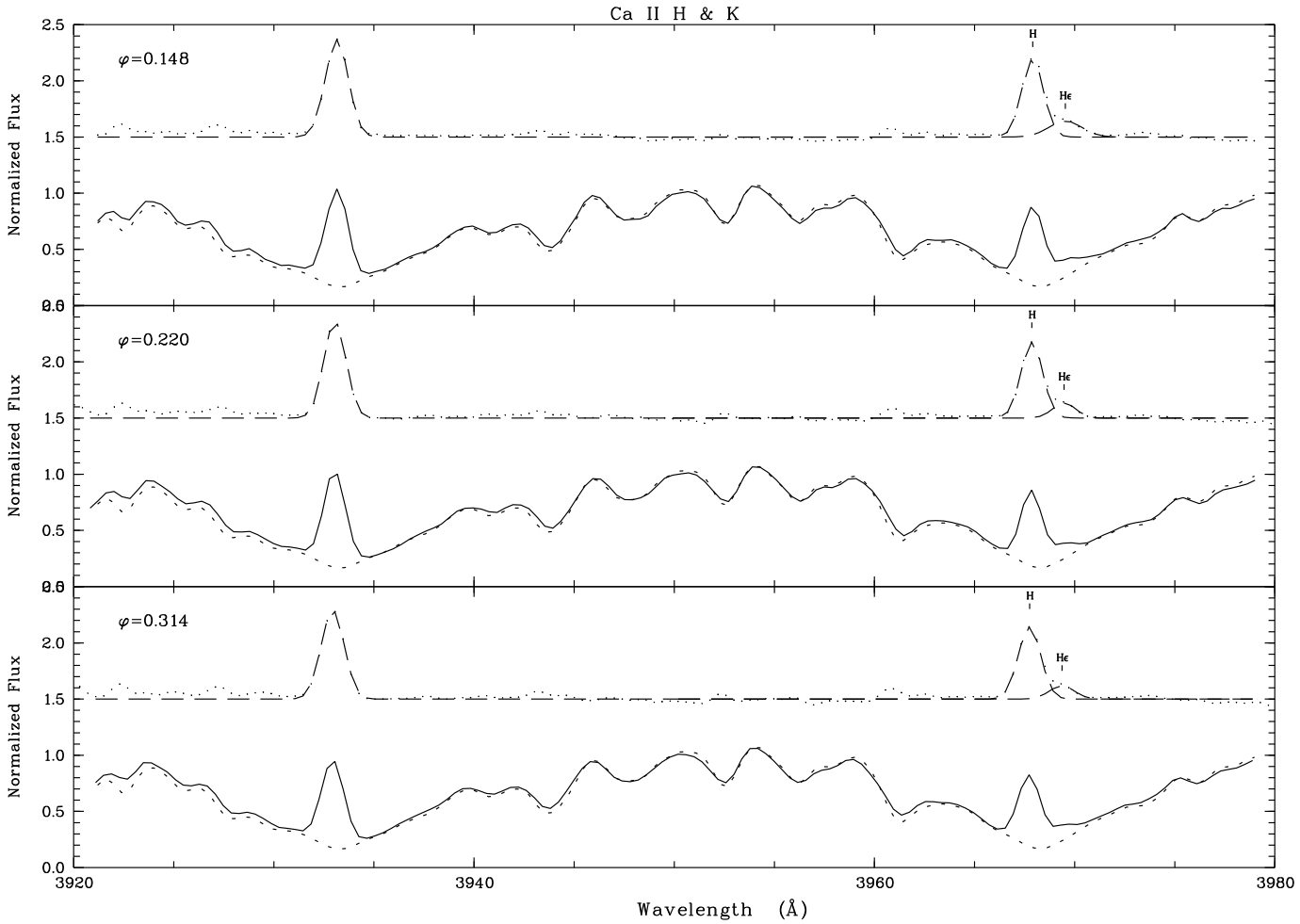

Fig. 9. INT/IDS Ca II H & K spectra (Nov 1996), as in Fig. 6

broad component to the total EW is larger in the λ8662 line. In the subtracted spectrum the intensity of the λ8498 line is higher than in λ8662; however, due to the contribution of the broad component, the total excess emission EW is larger in the λ8662 line.

5. Conclusions

In this paper we have analysed, using the spectral subtraction technique, simultaneous spectroscopic observations of several optical chromospheric activity indicators, at different epochs, of the RS CVn binary system EZ Peg.

We have found the Hα line in emission above the continuum in all the spectra, with noticeable changes in the line profile, that in part are due to the superposition of the absorption line to the other component. The subtracted Hα profile is well matched using a two-components Gaussian fit (narrow and broad). The broad component is mainly responsible for the observed variations of the subtracted profile, and its contribution to the total EW increases with the degree of activity. We have interpreted this broad component (also observed in other active systems in Paper I) as arising from microflaring activity that take place in the chromosphere.

A filled-in in the Hβ line has been found; however, the subtracted profiles do not present broad wings. The ratio ($E_{H\alpha}/E_{H\beta}$) that we have found indicates that the emission would arise from extended regions viewed off the limb.

Strong Ca II H & K emission from the hot component is observed in our spectra. The spectral subtraction reveals also a small but clear emission in the Hϵ line. The lines λ8498 and λ8662 of the Ca II IRT also show a strong emission. As in the case of the Hα line the subtracted profiles of these lines are well matched using a two-component Gaussian fit.

We suggest that the He I D_3 could present a total filling-in due to microflaring. We have not found filled-in by chromospheric emission in the Na I D_1 and D_2 lines nor in the Mg I b triplet lines.

All the activity indicators analysed here indicate that the hot component is the active star of the system, contrary to the usual behaviour observed in chromospherically active binaries. The variations (in different epochs and with the orbital phase)

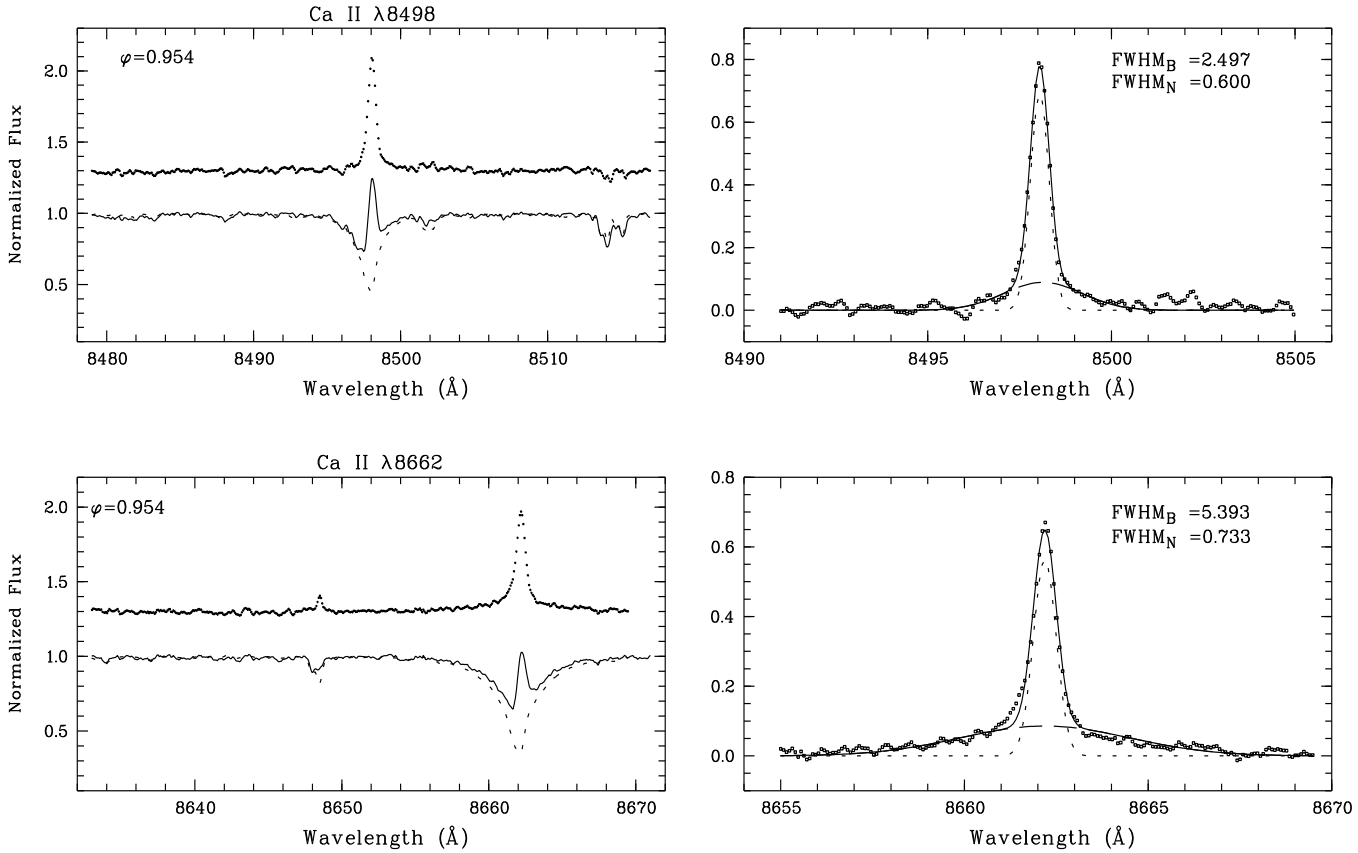

Fig. 10. WHT/UES Ca II IRT λ 8498 and λ 8662 spectra (Jul 1993), as in Fig. 3

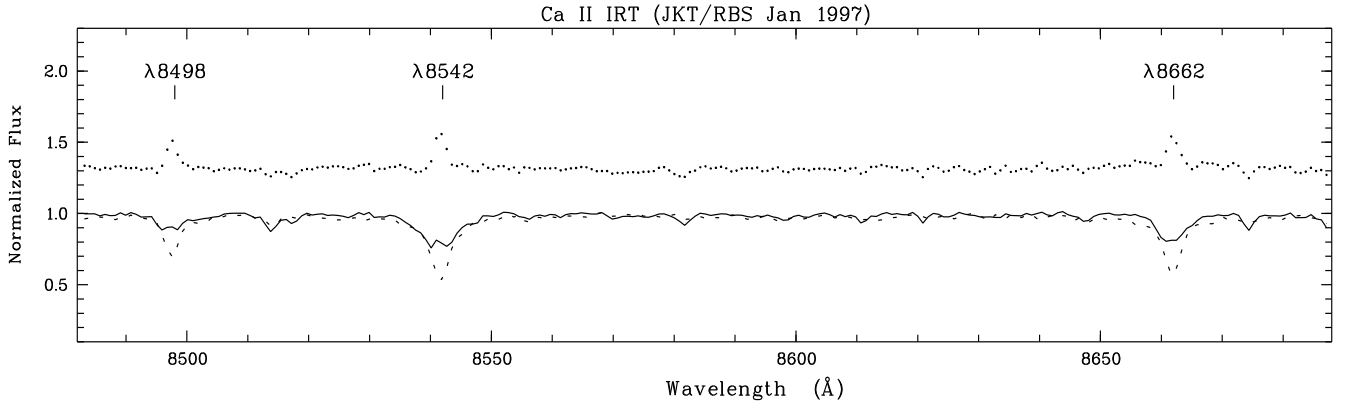

Fig. 11. JKT/RBS Ca II IRT spectrum (Jan 1997) at orbital phase 0.511

observed in the different indicators, formed at different heights in the chromosphere, are correlated.

The analysis of several Ti I lines with a positive effect in luminosity class indicates that the hot component is not a main sequence star but a subgiant or even of higher luminosity class, in contrast with the cool component that seems to be a dwarf. This result is confirmed by the application of the Wilson-Bappu effect to our Ca II K spectra. This difference in luminosity class, and therefore in convective zone depth, between the hot and cool components could explain why the hot component is the active star of the system.

Acknowledgements. We thank N. Cardiel and J. Cenarro for having taken and reduced the 1997 JKT spectrum. This research has made use of La Palma Archive. This work has been supported by the Universidad Complutense de Madrid and the Spanish Dirección General de Investigación Científica y Técnica (DGICYT) under grant PB94-0263.

References

Alden H.L., 1958, AJ, 63, 358
Andretta V., Giampapa M.S., 1995, ApJ 439, 405
Barrado D., Fernández-Figueroa M.J., García López R.J., De Castro, E., Cornide M., 1997, A&A 326, 780
Barret P., 1996, PASP 108, 412
Basri G., Wilcots E., Stout N., 1989, PASP 101
Cardiel N., Gorgas J., 1997 (in preparation)
Dempsey R.C., Bopp B.W., Henry G.W., Hall D.S., 1993, ApJS 86, 293
Dempsey R.C., Neff J., Linsky J.L., Brown A., 1996a, IAU Symp. 176, K.G. Strassmeier & J.L. Linsky (eds.), Stellar Surface Structure, p. 411
Dempsey R.C., Neff J., Thorpe M.J., et al., 1996b, ApJ 470, 1172
Favata F., Barbera M., Micela G., Sciortino S., 1993, A&A 277, 428
Fernández-Figueroa M.J., Barrado D., De Castro E., Cornide M., 1993, A&A 274, 373
Fernández-Figueroa M.J., Montes D., De Castro E., Cornide M., 1994, ApJS 90, 433
Foing B., Crivellari L., Vladilo G., Rebolo R., Beckman J., 1989, A&AS 80, 189
Ginestet N., Carquillat J.M., Jashek M., Jashek C., 1994, A&AS 108, 359
Griffin R.F., 1985, The Observatory, 105, 81
Gunn A.G., Hall J.C., Lockwood G.W., Doyle J.G., 1996, A&A 305, 146
Gunn A.G., Doyle J.G., 1997, A&A 318, 60
Gunn A.G., Doyle J.G., Houdebine E.R., 1997, A&A 319, 211
Hall J.C., Ramsey L.W., 1992, AJ 104, 1942
Hall J.C., 1996, PASP 108, 313
Howell S.B., Bopp B.W., 1985, PASP 97, 72
Howell S.B., Williams W.M., Barden S.C., Bopp B.W., 1986, PASP 98, 777
Huenemoerder D.P., Ramsey L.W., 1987, ApJ 319, 392
Huenemoerder D.P., Ramsey L.W., Buzasi D.L., 1990, Cool star stellar systems and the Sun, Sixth Cambridge Workshop., G. Wallerstein ed., ASP Conference Series 9, p 236
Irvine N.J., 1972, PASP 84, 671
Jashek C., Jashek M., 1995, "The Behavior of chemical elements in stars", Cambridge University Press
Keenan P.C., Hynek J.A., 1945, ApJ 101, 265
Kirkpatrick J.D., Henry T.J., McCarthy D.W., Jr., 1991, ApJS 77, 417
Linsky J.L., Hunten D., Glacken D., Kelch W., 1979, ApJS 41, 481
Linsky J.L., Wood B.E., 1994, ApJ 430, 342
Linsky J.L., Wood B.E., Judge P., Brown A., Andrulis C., Ayres T.R., 1995, ApJ 442, 381
Lutz T.E. 1970, AJ 75, 1007
Mihalas D., 1978, in Stellar Atmospheres, 2d ed. (San Francisco: Freeman), 381
Mitrou C.K., Doyle J.G., Mathioudakis M., Antonopoulou E., 1996, A&AS 115, 61
Montes D., Fernández-Figueroa M.J., De Castro E., Cornide M., 1994, A&A 285, 609
Montes D., Fernández-Figueroa M.J., De Castro E., Cornide M., 1995a, A&A 294, 165
Montes D., Fernández-Figueroa M.J., De Castro E., Cornide M., 1995b, A&AS 109, 135
Montes D., De Castro E., Fernández-Figueroa M.J., Cornide M. 1995c, A&AS 114, 287
Montes D., Fernández-Figueroa M.J., De Castro E., Cornide M. 1995d, Stellar Surface Structure, IAU Symp 176, Poster Proceedings, Strassmeier K. (ed), p. 167
Montes D., Fernández-Figueroa M.J., Cornide M., De Castro E., 1996a, A&A 312, 221
Montes D., Sanz-Forcada J., Fernández-Figueroa M.J., Lorente R., 1996b, A&A 310, L29
Montes D., Martín E.L., Fernández-Figueroa M.J., Cornide M., De Castro E. 1997a, A&AS 123, 473
Montes D., Fernández-Figueroa M.J., De Castro E., Sanz-Forcada J., 1997b, A&AS 125 (in press) (Paper I)
Pallavicini R., Cerruti-Sola M., Duncan D.K., 1987, A&A 174, 116
Pasquini L., Pallavicini R., Pakull M., 1988, A&A 191, 253
Pasquini L., Pallavicini R. 1991, A&A 251, 199
Robinson R.D., Airapetian V.S., Maran S.P., Carpenter K.G., 1996, ApJ 469, 872
Saar S.H., Huovelin J., Osten R.A., Shcherbakow A.G., 1997, A&A 326, 741
Schlesinger F., Barney I., Gesler C., 1934, Yale Trans., 10, 170
Schmidt-Kaler T. 1982, in Landolt-Börnstein, Vol. 2b, ed K. Schaifers, H.H. Voig (Heidelberg: Springer)
Shine R.A., Linsky J.L., 1972, SoPh, 25, 357
Shine R.A., Linsky J.L., 1974, SoPh, 39, 49
Soderblom D.R., Oey M.S., Johnson D.R.H., Stone R.P.S., 1990, AJ 99, 595
Strassmeier K.G., Hall D.S., Fekel F.C., Scheck M., 1993, A&AS 100, 173 (CABS)
Szkody P., 1977, ApJ 217, 140
Szkody P., Michalsky J.J., Stokes G.M., 1982, PASP 94, 137
Vilkki E.U., Welty D.E., Cudworth K.M., 1986, AJ 92, 989
Vyssotsky A.N., Balz A.G.A., 1958, Leander McCormick Publ., 13, 79
Wilson O.C., Bappu M.K.V. 1957, ApJ 125, 661
Wood B.E., Harper G.M., Linsky J.L., Dempsey R.C., 1996, ApJ 458, 761
Wood B.E., Linsky J.L., Ayres T.R., 1997, ApJ 478, 745
Zuiderwijk E.J., Martin R., Raimond E., van Diepem G.N.J. 1994, PASP 106, 515.

This article was processed by the author using Springer-Verlag LaTeX A&A style file *L-AA* version 3.